Molecular Dynamics Study on the Binding of *S*- and *R*-Ofloxacin to [d(ATAGCGCTAT)]$_2$ Oligonucleotide: Effects of Protonation States

Gi Nam Koo, Byung Hwa Lee, Sung Wook Han,† Seog K. Kim, and Hyun Mee Lee*

Department of Chemistry, College of Sciences, Yeungnam University, Gyeongsan, Gyeongbuk 712-749, Korea
**E-mail: wbhyun@yumail.ac.kr*
†*School of Herb Medicine Resource, Kyungwoon University, Gumi, Gyeongbuk 730-739, Korea*
Received August 20, 2008

The energies for the complex formation between the *S*- and *R*-enantiomers of ofloxacin with the [d(ATAGCGCTAT)]$_2$ were calculated using the molecular dynamics (MD) method. The 12 initial structures that were investigated in this work included were three ofloxacin: neutrals; zwitterions; and the protonated species, for both the *S*- and *R*-enantiomers, each with two starting positions intercalative and minor groove. The four final structures with the most favorable free energies from the MD calculations consisted of two categories namely, partial intercalative and the minor groove binding model. In the intercalative model that is found for the protonated species, the molecular plane of both the *S*- and *R*-ofloxacin is inserted between two GC base-pairs with the protonated piperazine ring and the methyl group of the oxazine ring is exposed to the minor groove. The binding energy of the *S*-ofloxacin in this model is slightly more favorable than *R*-ofloxacin. Conversely, even as it began with an initial intercalative structure, the neutral ofloxacin species is bound within the minor groove, whereby the molecular plane of ofloxacin tilts between 60-70° with respect to the DNA helical axis. Two hydrogen bonds are possible for this groove binding model. Finally, the free energy of the zwitterionic ofloxacin is less favorable than that obtained from neutral and protonated species.

Key Words : Molecular dynamics, Ofloxacin, Quinolone, DNA, Binding mode

Introduction

Quinolone antibiotics exhibit antibacterial activity by inhibiting the action of Topoisomerase II.[1] Interaction of norfloxacin and ofloxacin, representatives of the quinolone antibiotics, with DNA has been studied in order to understand the inhibition mechanism of these antibiotics[2-15] since it was originally proposed to bind to DNA, not protein.[14] However, ciproxacin, one of the quinolone derivatives, was known to affect the conformation of DNA gyrase.[16] In the presence of Mg^{2+} ions, norfloxacin was suggested to form an adduct by ligating the carboxylic and carbonyl groups to Mg^{2-} ions, with two negatively charged DNA phosphate groups participating in the complex.[6] Recently, it has been shown by spectroscopic studies that norfloxacin can directly bind to DNA without Mg^{2+} ion mediation with a preference for single-stranded DNA rather than double-stranded. When norfloxacin associated with double-stranded DNA, guanine is the preferred base, suggesting that its amine group that protrudes into the minor groove plays an important role in the quinolone-DNA adduct formation in the absence of Mg^{2-} ions.[10] The angle between the molecular plane of norfloxacin and the DNA helical axis was shown to be 67-80° when norfloxacin forms the complex with DNA, the complex between them in the absence of Mg^{2+} ion.[6-11]

Ofloxacin has a tricyclic ring structure with a methyl group at the C-3 position of the oxazine ring, which resulting in a chiral center. The *S*-ofloxacin was reported 8-128 times more potent than the *R*-isomer.[17] The binding properties of the *S*- and *R*-enantiomers towards DNA were studied and it was found that the binding mode and base specificity of *S*-ofloxacin to DNA was similar to those of norfloxacin, whereas the *R*-ofloxacin did not bind to DNA as efficiently.[10,11] In order to elucidate the chiral selectivity in the complex formation between ofloxacin and DNA, the structure of the ofloxacin-DNA complex was investigated by molecular modeling (MM) and molecular dynamics (MD).[18] In the complex, ofloxacin is located in the minor groove and forms two hydrogen bonds with two consecutive GC base pairs: one between the carbonyl group of ofloxacin and the amine group of guanine and the other between the fluorine of ofloxacin and the amine group of the next guanine at the opposite strand. The methyl group at the C-3 position of the oxazine ring is directed downward in the case of *R*-ofloxacin case, creating a closer distance to the phosphate backbone compared to the *S*-enantiomer whose methyl group is directed upward. This difference in the steric hindrance is the conceivable reason for the different binding affinities of these two stereoisomers toward DNA.

In the aqueous solution, quinolones, including ofloxacin, can have various protonation states (Figure 1). At a low pH, the nitrogen atom is protonated and the overall charge of ofloxacin is +1, while at intermediate pHs, ofloxacin is neutral which may be equilibrated with its zwitterion whose carboxylic moiety is deprotonated and piperazine ring is protonated. These three species of ofloxacin may be able to form an adduct with DNA. In this work, the bindings of these three species of *S*- and *R*-ofloxacin to DNA are studied by the molecular dynamic method. A high pH form at which carboxylic moiety may be deprotonated and the overall

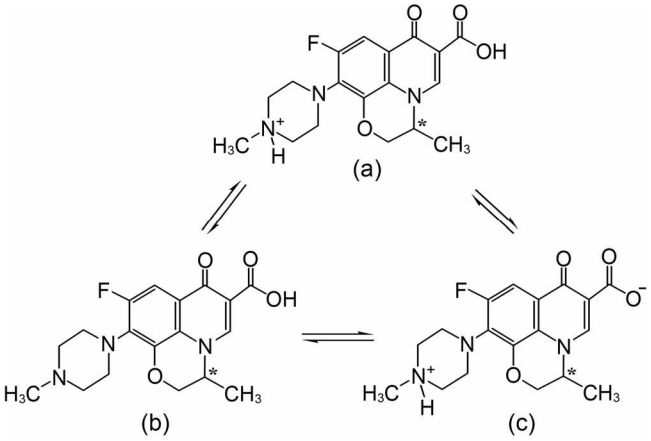

Figure 1. Chemical structures of (a) protonated ofloxacin; (b) neutral ofloxacin; and (c) zwitterionic ofloxacin.

charge of the molecule is −1 was not considered as it would not efficiently bind DNA due to repulsive forces between the negative charges of the ofloxacin and the DNA phosphate groups.

Methods

Modeling of the ofloxacin-DNA complexes. The six ofloxacin isomers were optimized using the HF/6-31G* basis set with the Gaussian 98 program package.[19] The B-form, double-stranded decanucleotide, $[d(ATAGCGCTAT)]_2$ was used for the modeling. The structures of the decamer and DNA-ofloxacin complexes were constructed with the nucleic acid in the Hyperchem7.0 program.[20]

The starting structures of the ofloxacin-DNA complexes were built by considering experimental[10,11] and theoretical evidences[13,18] that suggest that both *S*- and *R*-ofloxacin may sit in the minor groove with the possibility of partial intercalation when it forms a complex with DNA. Therefore, two starting structures namely, the partial intercalation and the minor groove binding mode, were considered for each forms of ofloxacin in this work. In the initial structures of the intercalation model, the molecular plane of the ofloxacin is parallel with the DNA base plane: the long molecular axis which connects the carbon atom of the carboxylic acid and nitrogen atom at the piperazine group angles 45 degrees with respect to the axis connecting phosphate groups of the opposite strands. In the initial structures of the minor groove binding model, the angle between the long molecular axis of ofloxacin and the DNA helical axis is 45 degrees with the carboxylic acid-fluorine side towards the DNA helix axis. Total starting structures had 12 models to account for ofloxacin conditions, binding modes, and isomers.

The nomenclature of the model structures is summarized in Table 1. The first characters, "s" and "r", indicate the *S*- and *R*-conformations of ofloxacin. The second and third characters, "in" or "g", indicate intercalation or minor groove binding. The final characters, "n", "p", and "z" represent the acidic state of the ofloxacin according to pH, denoting neutral, protonated, and zwitterionic, respectively.

Table 1. Nomenclature (in this work) for the ofloxacin-DNA complexes in the model structures

Binding mode	States of ofloxacin	*R*-ofloxacin	*S*-ofloxacin
Intercalation mode	neutral	rinn	sinn
	zwitterion	rinz	sinz
	protonated	rinp	sinp
Groove binding mode	neutral	rgn	sgn
	zwitterion	rgz	sgz
	protonated	rgp	sgp

Force Field. Molecular dynamics were performed using the AMBER 7.0 program package,[21] the Cornell *et al.* force field,[22] and the parm99.dat parameter set.[23] The generalized AMBER force field (GAFF) was used as the force field parameter of ofloxacin. The partial atomic charges for the ofloxacin molecules were calculated by the Gasteiger method. The Gasteiger approach,[24] in the estimation of electrostatics state of the ligands and ofloxacin in the current case, provides a more accurate estimation for binding affinities of the zwitterions, with a narrower range of computed affinities than that estimated by the RESP-based charge calculations.

Molecular dynamics. The DNA starting model was neutralized with 18 Na^+ ions and solvated with explicit water using the LEAP module of AMBER. The system was solvated with TIP3P water boxes requiring a 9.0 Å solvent shell in all directions. The number of waters in the periodic box was 2993-3514. The long-range electrostatic interactions are considered by applying the Ewald's particle mesh (PME) method.[25,26] All energy minimizations and molecular dynamics simulations were performed using the SANDER module. In the first step, 1000 steps of the steepest descent minimization followed by 1000 steps of conjugate gradient minimization were conducted for the water molecules and sodium ions with 500 kcal/mol·$Å^{-2}$ restraints placed on the DNA duplex. In the second step, 2000 steps of the steepest descent minimization followed by 3000 steps of conjugate gradient minimization were carried out for the whole system without restraints. The SHAKE algorithm[27] was applied to constrain all bonds involving hydrogen atoms with a tolerance of 10^{-5} Å, with a 2 fs time step in the dynamics simulations. The system was heated from 0 to 300 K over 100 ps with a 10 kcal/mol·$Å^{-2}$ restraint on the DNA at a constant volume, using the Berendsen coupling algorithm.[28] Finally, simulation of the whole system was performed at atmospheric pressure and 300 K with a 1.0 ps coupling parameter for 3 ns. No constraint was applied to the complexes. Three-dimensional structures and trajectories were visually inspected using the computer graphics program VMD.[29] Root mean-square deviations (RMSD) from the initial structures from the trajectories were calculated using the PTRAJ modules of AMBER 7.0. The backbone torsion angles of DNA were analyzed by the CURVES program.[30] All calculations were carried out on an IBM p690 system in the supercomputer center of the Korea Institute of Science and Technology Information (KISTI, Daejon, South Korea).

Free energy analyses. The molecular mechanics Generali-

zed Born surface area (MM-GBSA) method in AMBER was employed for thermodynamic analyses. This method allows for the estimation of the electrostatic free energies salvation of diverse molecules and molecular ions. In the GB model, a molecule in solution is represented as a set of point charges, set in spherical cavities, and embedded in a polarizable dielectric continuum. MM-GBSA is then able to calculate the relative stabilities of different conformations by dividing the total free energy into its single contributions. The free energies were estimated by final structures with water molecules and counterions removed. In the total model, the free energy consists of the internal energy (E_{gas}), the solvation free energy ($G_{GB} + G_{nonpolar}$), and the entropic contribution of the free energy. E_{int} contains the contributions of the all internal energy (bonds, angles, dihedral angles) and non-bonded (van der Waals, electrostatic, 1,4-electrostatic) interactions. The solvation free energy (G_{sol}) is divided into the electrostatic (G_{GB}) and nonpolar ($G_{nonpolar}$) parts. The free energies for each ofloxacin complex bound with the DNA duplex was computed with the equation: $G_{tot} = E_{gas} + G_{sol} - TS$. The solute entropic contribution was investigated by normal mode analysis using the NMODE module[31,32] in the AMBER package with the temperature set to 300 K. The binding free energies were calculated by the next following equation $\Delta G_{binding} = G_{complex} - (G_{DNA} + G_{ligand})$.

Results and Discussion

Optimized structures of various ofloxacin isomer. The structures of the six ofloxacins that depends on the protonation states and the configuration were optimized by Gaussian program. As it is shown in Figure 2, the oxazine ring puckers from the molecular plane which contains the two aromatic rings. The piperazine ring rotates to be perpendicular with respect to the molecular plane. In the optimized model, the axial position of the methyl group, relative to the oxazine ring and containing the chiral center, resulted in lower energy by 1.1-5.6 kcal/mol compared to those of the equatorial position. This result of relative stability between the position of methyl group, *i.e.*, equatorial *vs.* axial, was previously already reported for the neutral ofloxacin species.[18] The piperazine ring of all three protonated isomers rotated from the molecular plane and was almost perpendicular to the molecular plane. However, that of the neutral species tilted slightly towards the oxazine ring with the angle between the piperazine ring and the molecular plane slightly less than 90 degrees.

Table 2. The binding free energies of the ofloxacin-DNA complex (kcal/mol)

	R-ofloxacin	ΔG	*S*-ofloxacin	ΔG
neutral	rinn	−20.04	sinn	14.03
model	rgn	42.35	sgn	−21.26
zwitterion	rinz	−11.36	sinz	−10.72
model	rgz	3.22	sgz	14.52
protonated	rinp	−20.16	sinp	−24.64
model	rgp	−0.49	sgp	−7.35

Binding free energies of ofloxacin-DNA complex. The Root-mean square deviation (RMSD) is a good measure to judge whether the system reaches the equilibrium in the MD simulation. The system reached equilibrium within 200 ps for all complexes as it was judged by the RMSD (data not shown). The aforementioned, twelve initial complexes, two binding modes (intercalation *vs* minor groove binding) of the three species states for each enantiomer were constructed. The binding free energy, ΔG, was calculated using the MD simulation with the results are shown in Tables 2. The free energy for the binding of *S*-ofloxacin to the minor groove of DNA (the "sgn" initial structure) was the most favorable, being −21.26 kcal/mol among the neutral species. The intercalative binding mode of *R*-ofloxacin (the "rinn" initial structure) followed (−20.04 kcal/mol). In the case of the "rinn" initial structure, the MD dynamic calculation resulted in extrusion of the ofloxacin from the intercalation pocket into the minor groove. Although the favorable free energies were found for the zwitterionic ofloxacin for the "rinz" and "sinz" initial structures, the magnitude of the binding to DNA is significantly lower compared to the other ofloxacin conformations. The binding free energy for the "rinz" initial structure was −11.36 kcal/mol and that for the "sinz" was −10.72 kcal/mol. When the *N*-methyl group on the piperazine ring is protonated, the binding free energy is negative for all four binding modes suggesting that all

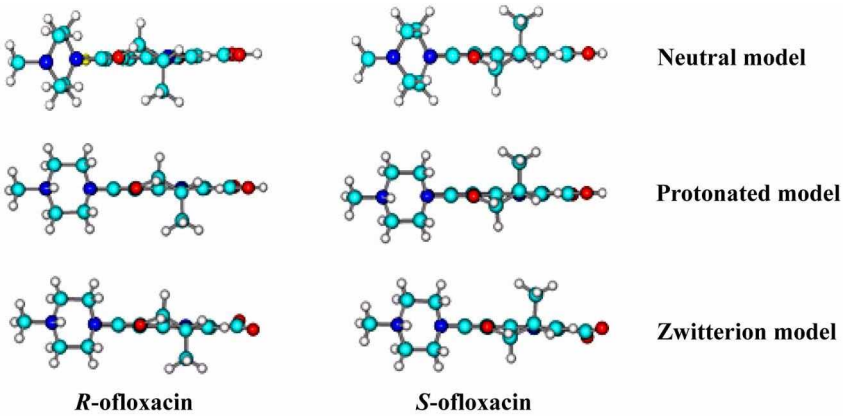

Figure 2. Optimized structures for the three protonated states of ofloxacin.

Table 3. Energy contributions (kcal/mol) of single trajectories. The contribution of DNA-free ofloxacin and ofloxacin-free DNA was subtracted from that of the complex

Energy	rinn	sgn	rinp	sinp
ΔE_{elec}	−992.93	−733.28	−708.26	−574.48
ΔE_{vdw}	−31.30	−41.44	−34.38	−51.91
ΔE_{int}	27.10	23.21	21.59	0.64
ΔE_{gas}	−980.24	−751.51	−721.04	−625.74
$\Delta G_{nonpolar}$	−1.63	−1.56	−1.25	−1.27
ΔG_{GB}	965.41	729.57	702.57	588.77
ΔG_{sol}	963.78	728.01	701.32	587.50
ΔG_{tot}	−18.46	−23.50	−19.72	−38.24
$T\Delta S_{tot}^{*}$	1.58	−2.24	0.44	−13.60
$\Delta G_{binding}$	−20.04	−21.26	−20.16	−24.64

*T: 298 K

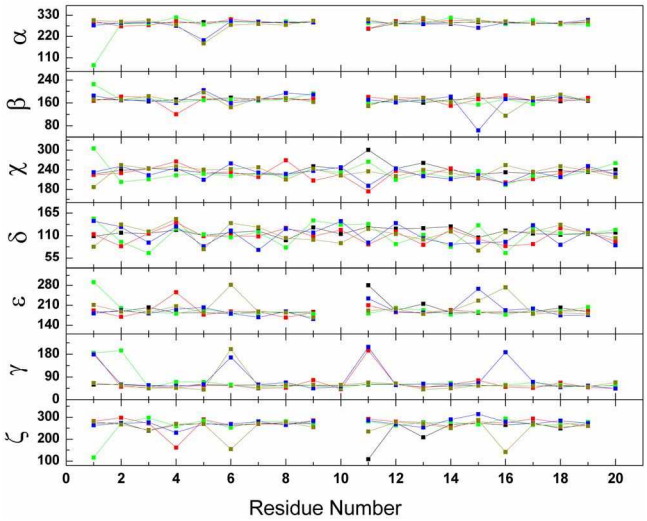

Figure 3. Backbone torsion angles for the oligonucleotide (black) and the final structures that resulted from the rinn (green), sgn (red), rinp (dark yellow), and sinp (blue) initial structures.

structures are not impossible. The "sinp" and "rinp" models were calculated at −24.64 kcal/mol and −20.16 kcal/mol, respectively, which are the two models that exhibited significantly stable binding energies thus two structures are conceivable for the protonated ofloxacin.

The experimental results showed that (1) the binding constant are larger at a lower pH compared to those at a higher pH[33], (2) both *S*- and *R*-ofloxacin can form a complex with GC-rich DNA[10,11] although the binding of the *R*-enantiomer is significantly less effective. Based on these experimental results and the free energy calculated in this work for the ofloxacin-oligonucleotide complex formation, the intercalative neutral ofloxacin ("rinn" and "sinn" initial structures) cannot explain the enantio-selectivity of ofloxacin because the formation free energy of the *S*-ofloxacin-oligonucleotide appeared to be unfavorable. In the minor groove binding model case, the free energy of the *S*-ofloxacin-oligonucleotide complex formation is lower than that of the *R*-enantiomer. However, that of the latter isomer exhibited the largest positive free energy which is in contrast with the experimental results that *R*-ofloxacin can form a complex with GC-rich DNA (although it is less effective than the *S*-enantiomer). The magnitudes of the free energies for the binding of zwitterionic ofloxacins to DNA that resulted from the intercalative initial structure ("rinz" and "sinz") are, in general, smaller than the other two forms of ofloxacin. Those for the groove binding model are small, but positive, relative to the experimental results. The intercalative initial binding model ("rinp" and "sinp") of the protonated ofloxacin exhibited the most conceivable results in the sense that the free energy for both enantiomers are negative and that the magnitude of the *S*-enantiomer is larger than *R*, although the difference is small. The magnitude obtained from the initial groove binding model of the protonated species ("rgp" and "sgp") are very small compared to intercalative model and therefore, its occurrence is not conceivable.

Table 3 shows the energy contributions of single trajectories to the total binding free energy of the four representative initial structures (that resulted in the large favorable free energy), from which the contribution from unbound ofloxacin and DNA were subtracted. The main contribution, in comparison with other initial structures, for the lowest free energy of the "sinp" initial structure is the lowest solvation energy, although the E_{gas} corresponding to non-bonded interactions of "sinp" model is noticeably high.

Structural analyses. Structural analysis was performed for the complexes "rinn", "sgn", "rinp", and "sinp" and resulted in a large favorable free energy with the backbone angles for these models shown in Figure 3. Intercalation of protonated ofloxacin to DNA, the model resulting from the "rinp" and "sinp" initial structures, resulted in large deviations in the α, β, γ, and ζ angles near the intercalation pocket near the C5 and G16, and G6 and C15 base pairs, in comparison with DNA in the absence of ofloxacin. The small deviations in the χ and δ are observable in the whole region of DNA. As it was mentioned above, the MD calculation for the "rinn" initial structure, in which *R*-ofloxacin is initially intercalated, resulted in extrusion of the ofloxacin from the intercalation pocket and is located in the minor groove of the final structure. The torsion angles near the binding site do not largely change from those of ofloxacin-free DNA, although a significant deviation was found at the end of one of the two double strands. No significant deviation in the backbone angle was noticed for the groove binding model that originated from the "sgn" initial structure. In conclusion, the backbone angles for all four models remained as the overall B-form DNA.

Figure 4 and 5 depict the stereo-views of the final structures of the two GC sequences near the ofloxacin binding site from which water, counter ions, and the three base pairs at both ends are omitted for clarity reason. In Figure 4, the ofloxacin molecule is neutral. For both started from intercalative *R*-ofloxacin and minor groove binding *S*-ofloxacin, which resulted two lowest binding free energy with minor groove binding mode. In the final structure, the angle of the molecular plane of ofloxacin including the two aromatic

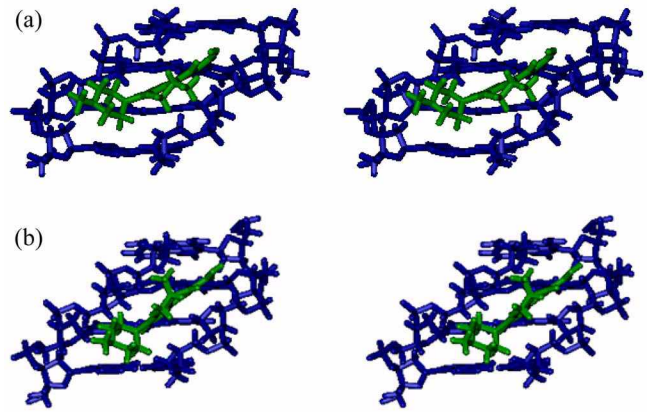

Figure 4. Stereoview of the models that originated from the "rinn" (a) and "sgn" (b) final structures after molecular dynamics simulation. The blue and green colors indicate DNA and ofloxacin.

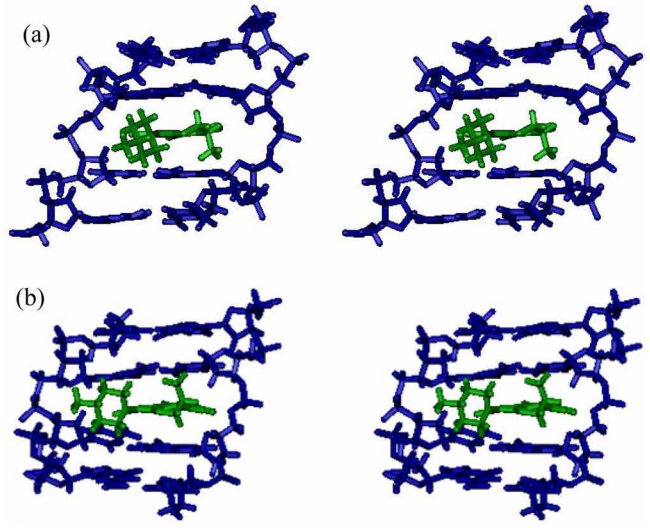

Figure 5. Stereoview of the models that originated from the "rinp" (a) and "sinp" (b) final structures after molecular dynamics simulation. The blue and green colors indicate DNA and ofloxacin.

rings are 60-70° relative to the DNA helical axis. As a result of the ofloxacin binding, the minor groove near the binding site becomes narrower and the DNA stem is bent, similar to previously reported results.[18] In the final structure that originated from the "rinp" initial structure (Figure 5a), the aromatic ring moiety of the ofloxacin molecule is inserted between the GC base pairs. The methyl group and piperazine ring protrude into the minor groove due to the steric hindrance, with the distance between the base pairs larger and wider as a result of the intercalation, which is typical for drug intercalation. It was also found that the minor groove near the center of the ofloxacin binding site becomes more shallow and the length of DNA near the methyl group of ofloxacin increases resulting in the bending of the DNA. The final structure from the "sinp" initial structure, shown in Figure 5b, appeared to have a deeper minor groove and a larger intercalation pocket compared to that from the "rinp" initial structure. The extent of DNA bending of the *S*-ofloxacin-DNA complex is larger due to the right-handedness of the DNA helix. The methyl group of the *S*-ofloxacin is directly right-upward which inducing a greater steric hindrance and in order to avoid this steric hindrance, larger bending in the DNA stem is expected for the *S*-ofloxacin-DNA complex.

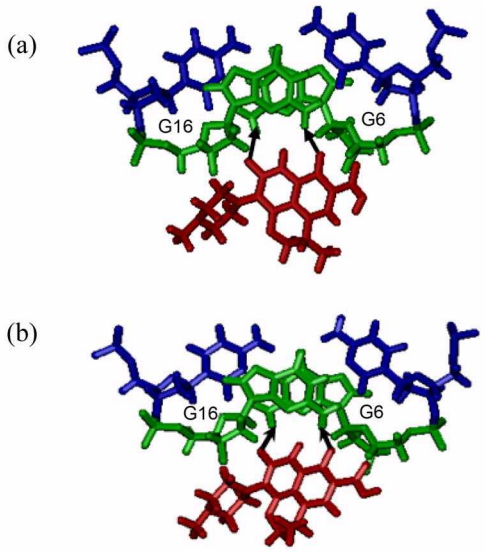

Figure 6. Top views of the "rinn" (a) and the "sgn" models (b). The black arrows indicate possible hydrogen bonds between oxygen in the carboxylic moiety of ofloxacin and the hydrogen atom of the G16 guanine amine group, and between the fluorine and the hydrogen atom of the G6 guanine amine group. Red, green and blue colors indicate ofloxacin, guanine, and cytosine, respectively.

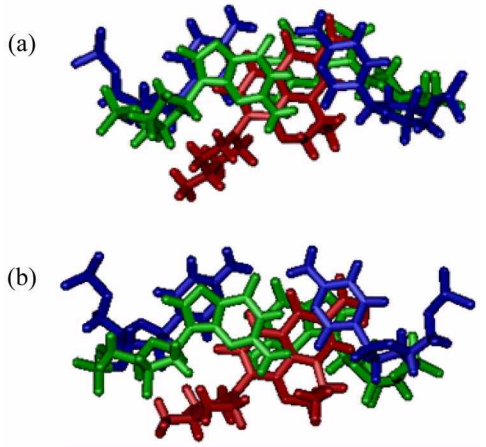

Figure 7. Top views of the "rinp" (a) and "sinp" (b) models. The color assignments are the same as in Figure 6.

The views from the top for the central two base pairs bound to which ofloxacin is bound are shown in the Figures 6 and 7. The neutral *R*-ofloxacin and *S*-ofloxacin associates with DNA in the minor groove (Figure 6a and 6b), originating from the intercalative "rinn" and minor groove binding "sgn" initial structures. It was noticed that the direction of the OH group of the carboxylic group is opposite in the final models. The two hydrogen bonds between the oxygen of the carboxylic moiety of ofloxacin and the hydrogen atom of the G16 guanine's amine group, and between the fluorine and

the hydrogen atom of the G6 guanine's amine group were found. The length of the two hydrogen bonds is 2.22 Å and 2.32 Å in the "rinn" model, while those are short in the "sgn" model are 2.03 Å and 1.85 Å. The binding strength between ofloxacin and DNA is expected to be stronger in the "sgn" model compared to that in the "rinn" model as bond length is directly related to the binding strength. This observation agrees with the experimental results that the binding of *S*-ofloxacin is more favorable than *R*-ofloxacin.[11] Figure 7a and 7b depict the top views of the final models constructed from the "rinp" and "sinp" initial structures, respectively, where in both models, it is clear that the aromatic rings of the both ofloxacin enantiomers is inserted between the GC base-pairs. The piperazine ring and methyl group of the oxazine ring are exposed in the minor groove. This result is in agreement with the recent NMR study that norfloxacin, another member of the quinolone antibiotics, is partially intercalated between DNA base pairs.[15]

Conclusion

Energetically favorable but different structures for the ofloxacin-DNA complex that depends on the protonated state of ofloxacin were observed in this work. The minor groove binding is preferred for the neutral ofloxacin while the partial intercalative models are more stable for the protonated species. The binding free energy of the zwitter ionic ofloxacin is less favorable compared to that of the neutral and protonated species. Of important note is the preferentiality in binding of the *S*-ofloxacin to DNA over the *R*-enantiomer and its significant in the neutral species and protonated model.

Acknowledgments. This work was supported by the Korea Research Foundation (Grant No. KRF-2005-050-C00003).

References

1. Hooper, D. C.; Wolfson, J. S. *Quinolone-Antimicrobial Agent*, 2nd ed.; American Society for Microbiology: Washington, DC, for review 1993.
2. Shen, L. L. *Biochemical Pharmacology* **1989**, *38*, 2042-2044.
3. Shen, L. L.; Kohlbrenner, W. E.; Weigi, D.; Baranowski, J. *J. Biol. Chem.* **1989**, *264*, 2973-2978.
4. Shen, L. L.; Mitscher, L. A.; Sharma, P. N.; O'Donnel, T. J.; Chu, D. W. T.; Cooper, C. S.; Rosen, T.; Pernet, A. G. *Biochemistry* **1989**, *28*, 3886-3894.
5. Palù, G.; Valisena, S.; Perachi, M.; Palumbo, M. *Proc. Natl. Acad. Sci. USA* **1992**, *89*, 9671-9675.
6. Son, G.-W.; Yeo, J.-A.; Kim, M.-S.; Kim, S. K.; Holmén, A.; Åkerman B.; Nordén, B. *J. Am. Chem. Soc.* **1998**, *120*, 6451-6457.
7. Son, G.-W.; Yeo, J.-A.; Kim, J.-M.; Kim, S. K.; Moon, H. R.; Nam, W. *Biophys. Chem.* **1998**, *74*, 225-236.
8. Yeo, J.-A.; Cho, T.-S.; Kim, S. K.; Moon, H. R.; Jhon, G.-J.; Nam, W. *Bull. Kor. Chem. Soc.* **1998**, *19*, 449-457.
9. Lee, E.-J.; Yeo, J.-A.; Lee, G-J.; Han S. W.; Kim, S. K. *Eur. J. Biochem.* **2000**, *267*, 6018-6024.
10. Lee, E.-J.; Yeo, J.-A.; Jung, K.; Hwangbo, H. J.; Lee, G-J.; Kim, S. K. *Arch. Biochem. Biophys.* **2001**, 395, 21-24.
11. Hwangbo, H. J.; Yun, B. H.; Cha, J. S.; Kwon, D. Y.; Kim, S. K. *Eur. J. Pharm Sci.* **2003**, *18*, 197-203.
12. Bailly, C.; Colson, P.; Houssier, C. *Biophys. Res. Commun.* **1998**, *243*, 844-848.
13. Lee, H. M.; Kim, J.-K.; Kim, S. K. *J. Biomol. Struct. Dyn.* **2002**, *19*, 1083-1091.
14. Shen, L. L.; Pernet, A. G. *Proc. Natl. Acad. Sci. USA* **1985**, *82*, 307-311.
15. Sandström, K.; Wärmländer, S.; Leijon, M.; Gräslund, A. *Biochem. Bioph. Res. Co.* **2003**, *304*, 55-59.
16. Sissi, C.; Perdonà, E.; Domenici, E.; Feriani, A.; Howells, A. J.; Maxwell, A.; Palumbo, M. *J. Mol. Biol.* **2001**, *311*, 195-203.
17. Hayakawa, I.; Atarashi, S.; Yokohama, S.; Imamura, M.; Sakano, K.-I.; Furukawa, M. *Antimicrob. Agents Chemother* **1986**, *29*, 163-164.
18. Lee, H. M.; Kim, H. D.; Kim, J. M.; Kim, J.-K.; Kim, S. K. *J. Biomol. Struct. Dyn.* **2007**, *25*, 231-241.
19. Frich, M. J.; Trucks, G. W.; Schlegel, H. B.; Scuseria, G E.; Robb, M. A.; Cheeseman, J. R.; Zakzewski, V. G; Montgomery, Jr. J. A.; Stratman, R. E.; Burant, J. C.; Dapprich, S.; Millam, J. M.; Daniels, A. D.; Kudin, K. N.; Strain, M. C.; Farkas, O.; Tomasi, J.; Barone, V.; Cossi, M.; Cammi, R.; Mennucci, B.; Pomelli, C.; Adamo, C.; Clifford, S.; Ochterski, J.; Petersson, G. A.; Ayala, P. Y.; Morokuma, Q.; Cui, K.; Malick, D. K.; Rabuck, A. D.; Raghavachari, K.; Foresman, J. B.; Cioslowski, J.; Stefanov, J. V.; Ortiz, B. B.; Liashenko, G; Liu, A.; Piskorz, P.; Komaromi, I.; Gomperts, R.; Martin, R. L.; Fox, D. J.; Keith, T.; Al-Laham, M. A.; Peng, C. Y.; Nanayakkara, A.; Gonzalez, C.; Challacombe, M.; Gill, P. M. W.; Johnson, B.; Chen, M. W.; Wong, J. L.; Andres, W.; Head-Gordon, M.; Replogle, E. S.; Pople, J. A. *Gaussian 98*, Revision A. 3.; Gaussian, Inc.: Pittsburgh, PA, 1998.
20. Case, D. A.; Pearlman, D. A.; Caldwell, J. W.; Cheatham, T. E. III.; Wang, J.; Ross, W. S.; Simmering, C. L.; Darden, T. A.; Merz, K. M.; Stanton, R. V.; Cheng, A. L.; Vincent, J. J.; Crowley, M.; Tsui, V.; Gohlke, H.; Radmer, R. J.; Duan, Y.; Pitera, J.; Massova, I.; Seibel, G. L.; Singh, U. C.; Weiner, P. K.; Kollman, P. A. AMBER7; University of California: San Francisco, 2002.
21. Case, D. A.; Pearlman, D. A.; Caldwell, J. W.; Cheatham, T. E. III.; Wang, J.; Ross, W. S.; Simmering, C. L.; Darden, T. A.; Merz, K. M.; Stanton, R. V.; Cheng, A. L.; Vincent, J. J.; Crowley, M.; Tsui, V.; Gohlke, H.; Radmer, R. J.; Duan, Y.; Pitera, J.; Massova, I.; Seibel, G. L.; Singh, U. C.; Weiner, P. K.; Kollman, P. A. *AMBER7*; University of California: San Francisco, 2002.
22. Cornell, W. D.; Cieplak, P.; Bayly, C. I.; Gould, I. R.; Merz, K. M.; Ferguson, D. M.; Spellmeyer, D. C.; Fox, T.; Caldwell, J. W.; Kollman, P. A. *J. Am. Chem. Soc.* **1995**, *117*, 5179-5197.
23. Cheatham, T. E.; Cieplak, P.; Kollman, P. A. *J. Biomol. Struct. Dyn.* **1999**, *16*, 845-862.
24. Bonnet, P.; Bryce, R. A. *J. Mol. Graph. Model.* **2005**, *24*, 147-156.
25. Essmann, U.; Perera, L.; Berkowitz, M. L.; Darden, T.; Lee, H.; Pedersen, L. G. *J. Chem. Phys.* **1995**, *103*, 8577-8593.
26. Darden, T.; York, D.; Pedersen, L. G. *J. Chem. Phys.* **1993**, *98*, 10089-10092.
27. Ryckaert, J. P.; Ciccotti, G.; Berendsen, H. J. C. *J. Comput. Phys.* **1977**, *23*, 327-341.
28. Berendsen, H. J. C.; Postma, J. P. M.; van Gunsteren, W. F.; DiNola, A.; Haak, J. R. *J. Chem. Phys.* **1984**, *81*, 3684-3690.
29. Humphery, F. W.; Dalke, A.; Shulten, K. *J. Mol. Graphics* **1996**, *14*, 33-38.
30. Laver, R.; Sklenar, H. *CURVES 5.3*, 1990.
31. Srinivasan, J.; Cheatham, T. E. III; Cieplak, P.; Kollman, P. A.; Case, D. A. *J. Am. Chem. Soc.* **1998**, *120*, 9401-9409.
32. Kollman, P. A.; Massova, I.; Reyes, C.; Kuhn, B.; Huo, S.; Chong, L.; Lee, M.; Lee, T.; Duan, Y.; Wang, W.; Donini, O.; Cieplak, P.; Srinivasan, J.; Case, D. A.; Cheatham, T. E. III. *Acc. Chem. Res.* **2000**, *33*, 889-897.
33. Yeo, J.-A.; Son, G-S.; Kim, J. M.; Jun, E. D.; Moon, H. R.; Cho, T.-S. *J. Kor. Chem. Soc.* **2000**, *44*, 4-9.